Electronic Supplementary Material (ESI) for Green Chemistry.
This journal is © The Royal Society of Chemistry 2025

Supplemental Information

Soft Glass Interphase Engineering for Ultra-stable Aluminum Metal Batteries

Shibin Zhang[1], Yan Xu[1], Danni Zhang[1], Lishun Bai[1], Yue Liu[1], Ying He[1], Feiyan Yu[1], Chengjun Liu[1], Sijie Li[2]*, Zhi Chang[1]*

Affiliations:

[1]School of Materials Science and Engineering, Key Laboratory of Electronic Packaging and Advanced Functional Materials of Hunan Province, Central South University, Changsha, 410083, Hunan, China.

E-mail: zhichang@csu.edu.cn (Prof. Z. C.)

Dr. S. Li

[2]College of Chemistry and Chemical Engineering, Central South University, Changsha 410083, Hunan, China.

E-mail: li.sijie@csu.edu.cn (Dr. S. L.)

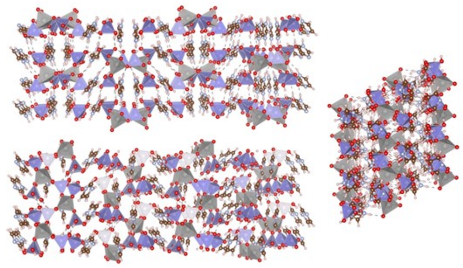

Figure S1. Schematic diagram of the microstructure of ZnP-H_2Im powder

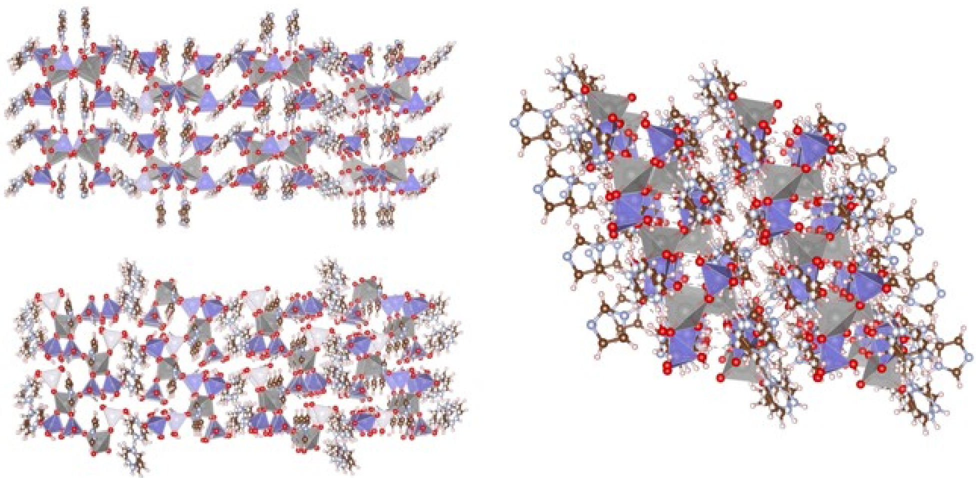

Figure S2. Schematic diagram of the microstructure of ZnP-H_2Im glass.

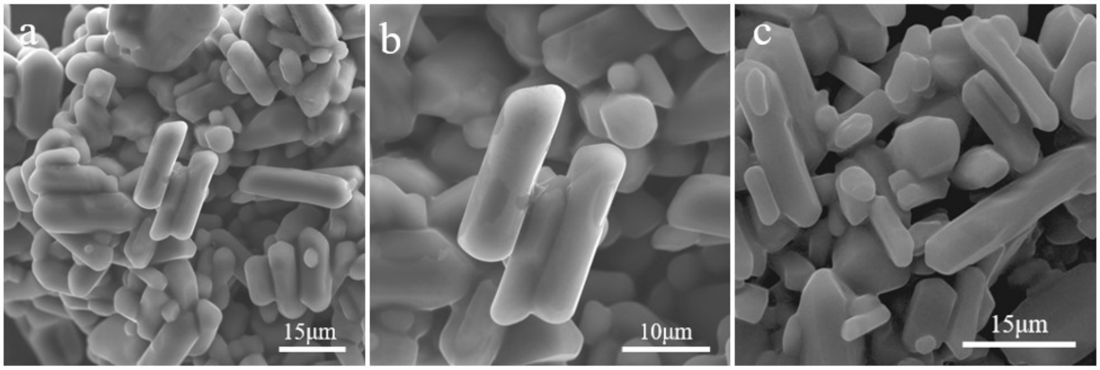

Figure S3. SEM image of ZnP-H_2Im powder.

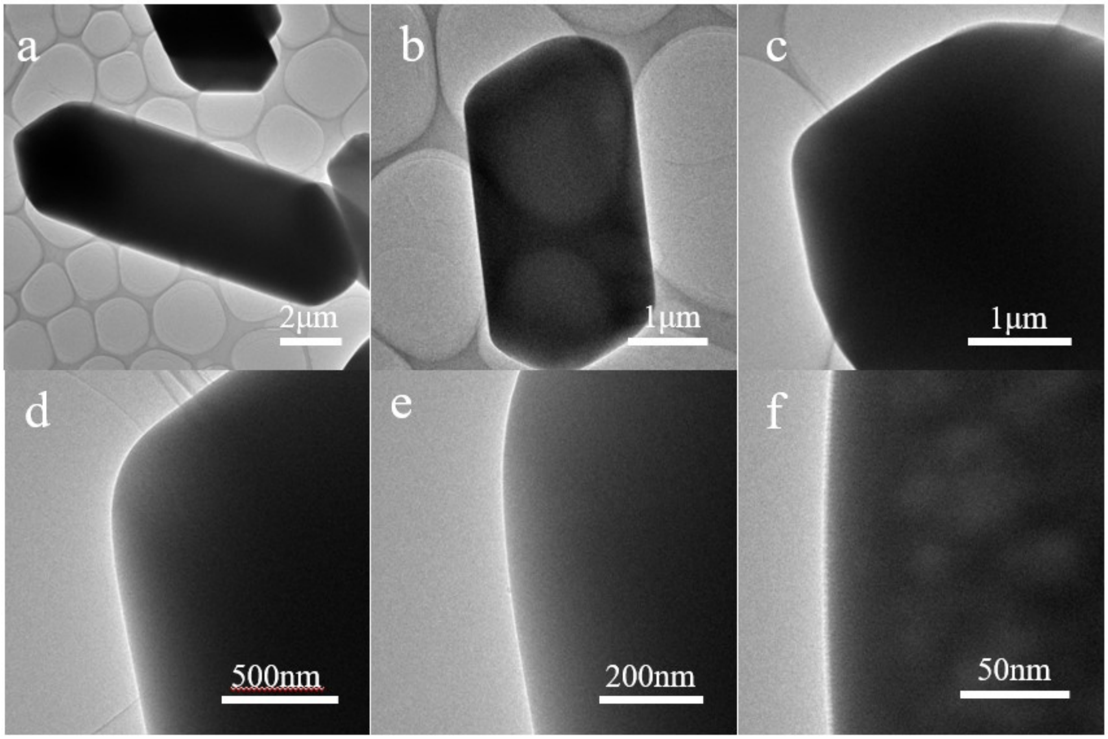

Figure S4. TEM image of ZnP-H_2Im powder.

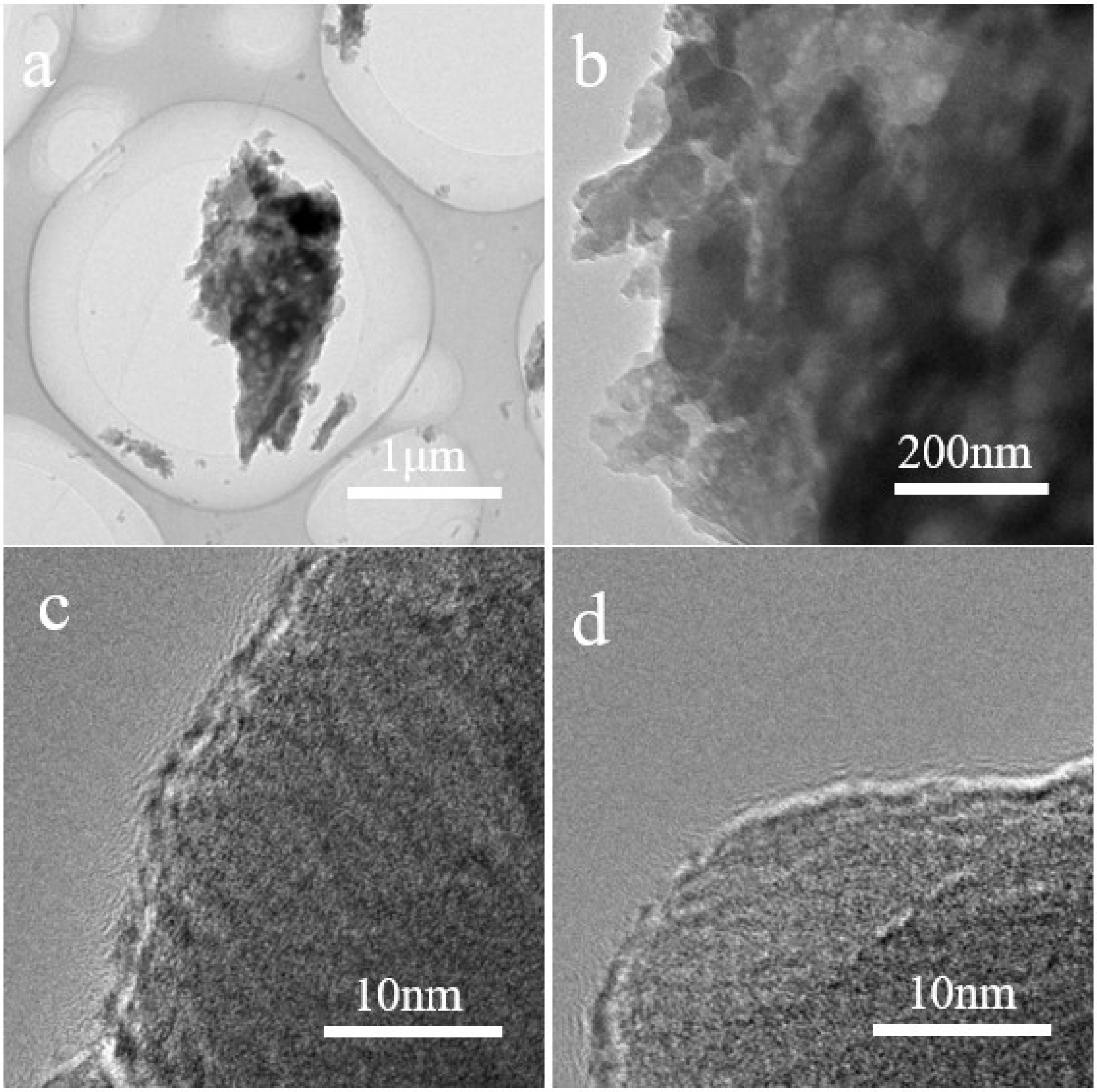

Figure S5. TEM image of ZnP-H_2Im glass.

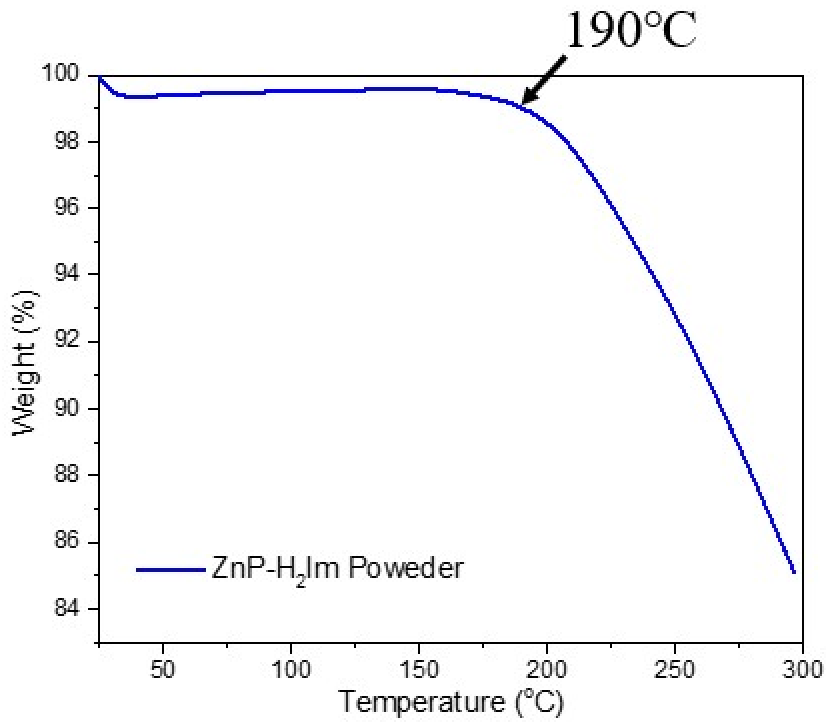

Figure S6. Thermogravimetric analysis (TGA) curve of ZnP-H_2Im powder.

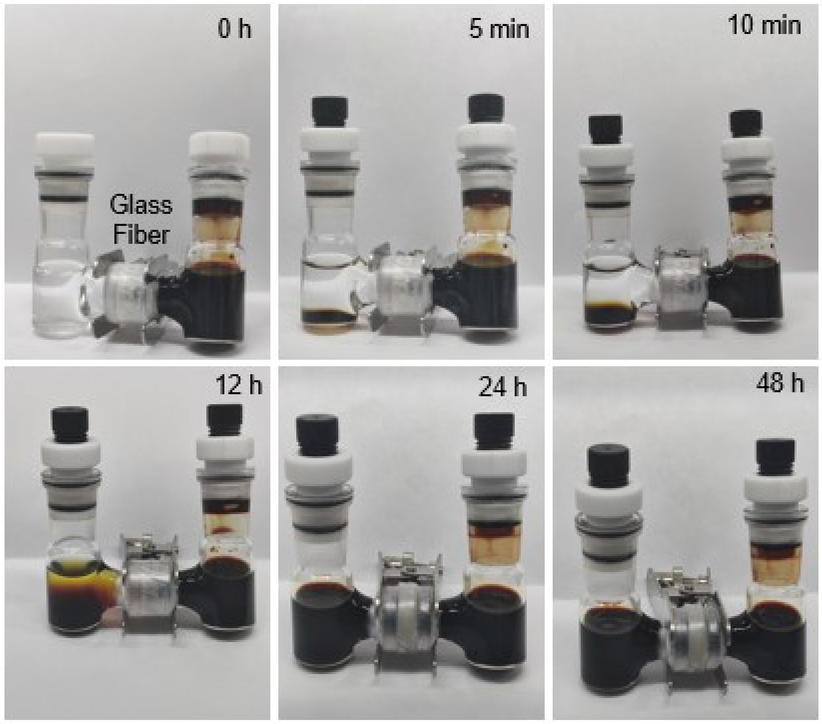

Figure S7. Photographs of the 0–48 hours permeation experiment using ZnP-H_2Im glass.

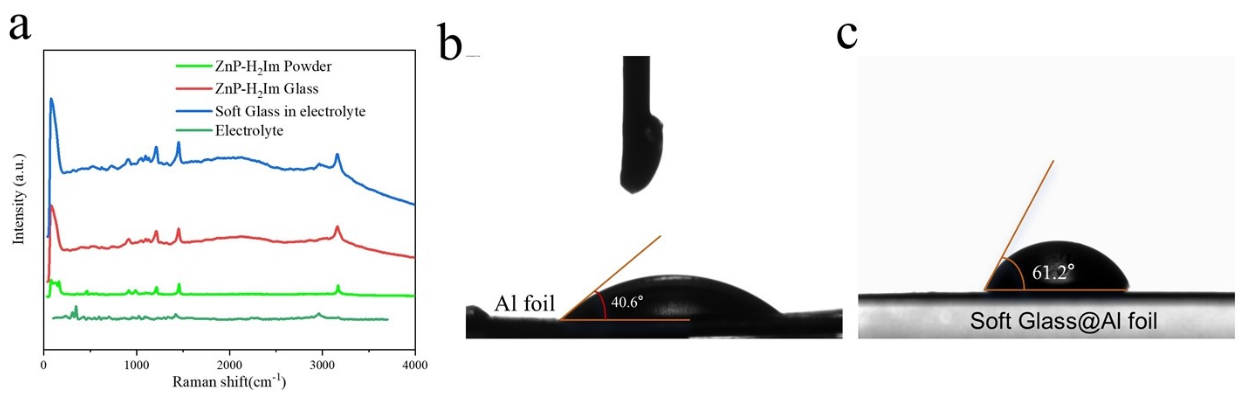

Figure S8. (a) Raman spectra of ZnP-H_2Im powder, ZnP-H_2Im glass, ZnP-H_2Im glass soaked in $AlCl_3$/[EMIm]Cl electrolyte for 12 hours, and $AlCl_3$/[EMIm]Cl electrolyte. (b) Contact angle photograph of $AlCl_3$/[EMIm]Cl droplet on Al foil. (c) Contact angle photograph of $AlCl_3$/[EMIm]Cl droplet on ZnP-H_2Im glass.

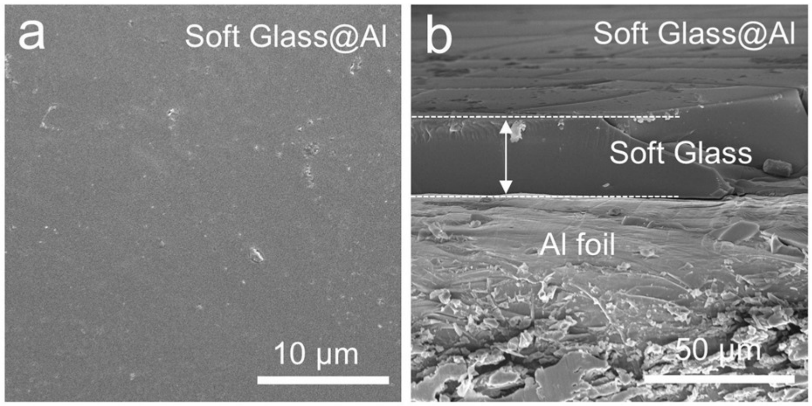

Figure S9. SEM images of the ZnP-H_2Im soft glass-coated aluminum foil: (a) top view and (b) cross-sectional view.

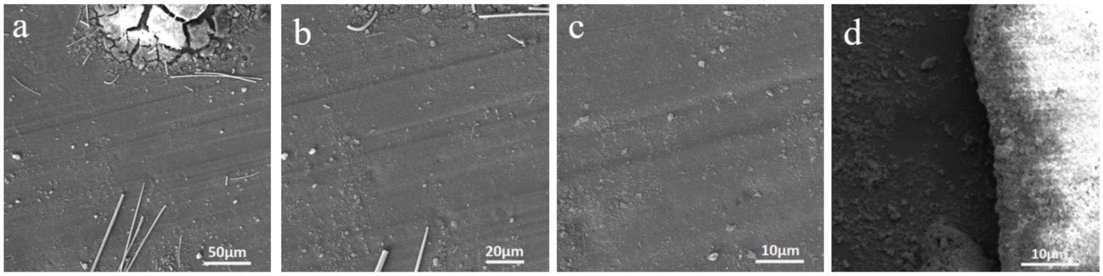

Figure S10. SEM image of the Al electrode surface from the ZnP-H_2Im@Al//ZnP-H_2Im@Al symmetric battery after cycling for 1200 hours at 0.1 mA/cm² and 0.1 mAh/cm², with the surface ZnP-H_2Im soft glass layer removed.

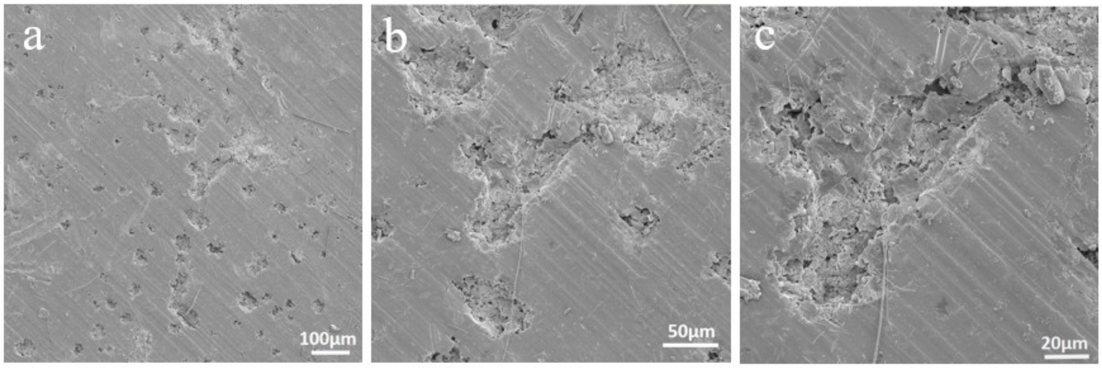

Figure S11. SEM image of the Al electrode surface from the Al//Al symmetric battery after cycling for 1200 hours at 0.1 mA/cm^2 and 0.1 mAh/cm^2.

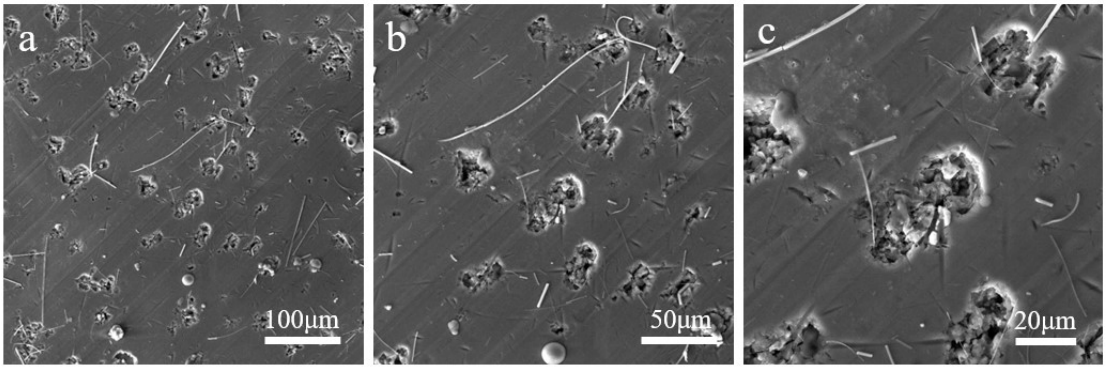

Figure S12. SEM image of the Al electrode surface from the Al//Al symmetric battery after cycling for 650 hours at 0.2 mA/cm^2 and 0.2 mAh/cm^2.

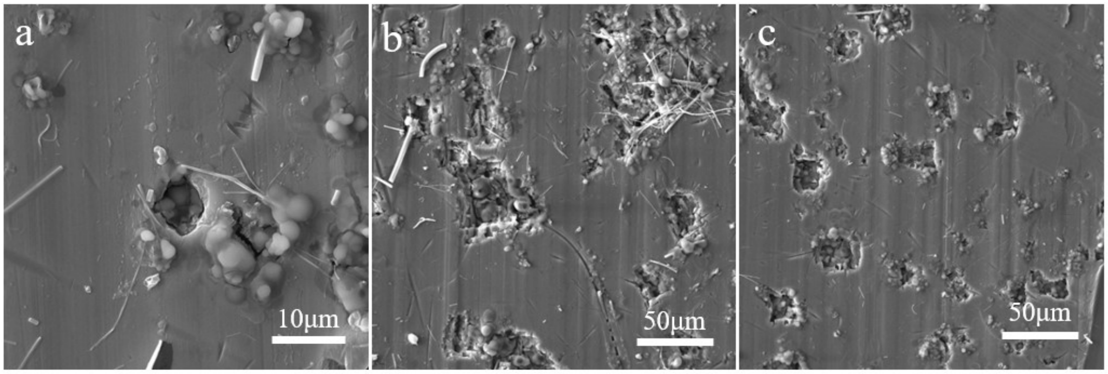

Figure S13. SEM image of the Al electrode surface from the Al//Al symmetric battery after cycling for 210 hours at 0.5 mA/cm² and 0.5 mAh/cm².

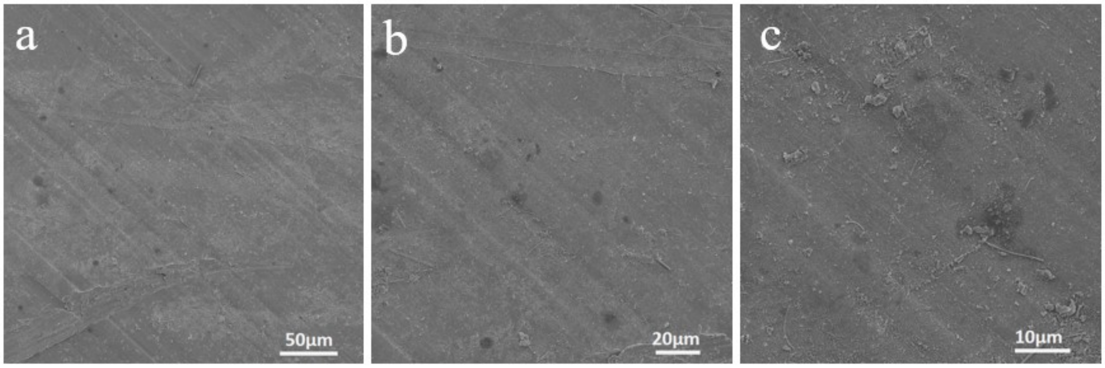

Figure S14. SEM image of the Al electrode surface from the ZnP-H_2Im@Al//ZnP-H_2Im@Al symmetric battery after cycling for 650 hours at 0.2 mA/cm² and 0.2 mAh/cm², with the surface ZnP-H_2Im soft glass layer removed.

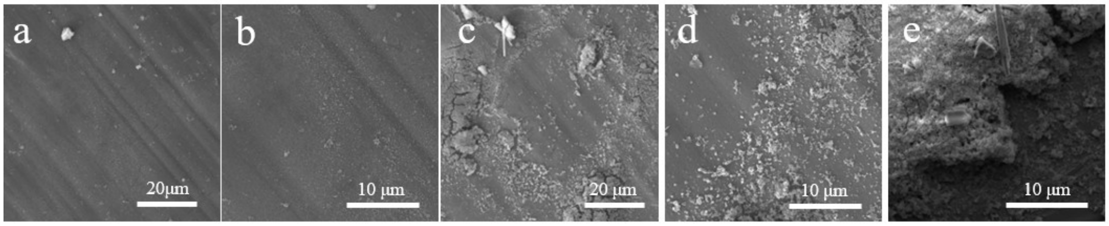

Figure S15. SEM image of the Al electrode surface from the ZnP-H_2Im@Al//ZnP-H_2Im@Al symmetric battery after cycling for 210 hours at 0.2 mA/cm² and 0.2 mAh/cm², with the surface ZnP-H_2Im soft glass layer removed.

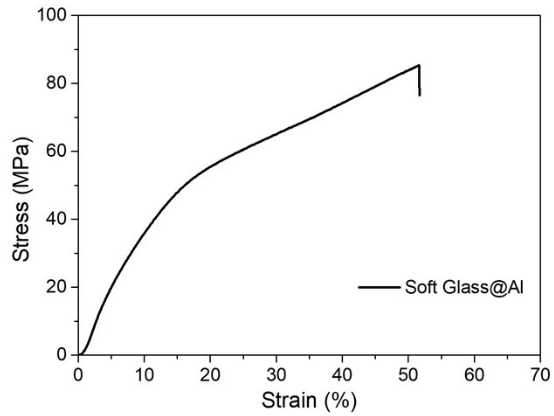

Figure S16. Stress-strain profiles of the ZnP-H_2Im glass.

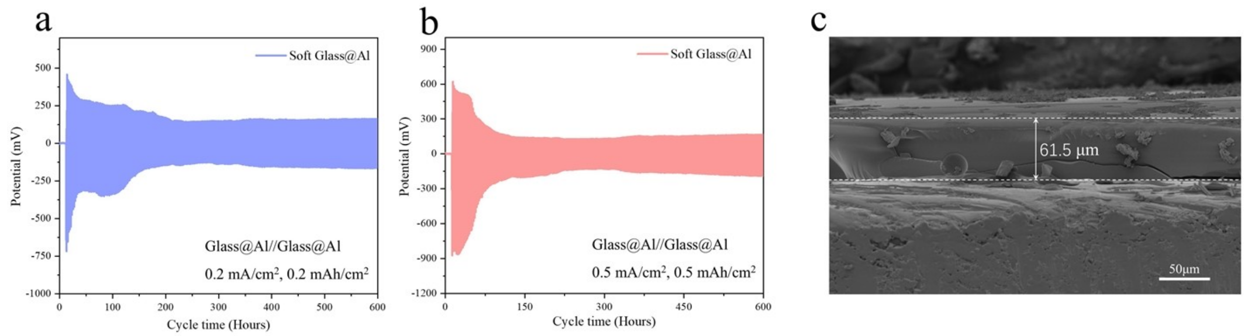

Figure S17. Long-term cycling performance and post-cycling characterization of ZnP-H_2Im@Al symmetric cells: (a) Cycling profiles at 0.2 mA/cm² and 0.2 mAh/cm², (b) profiles at 0.5 mA/cm² and 0.5 mAh/cm², (c) cross-sectional SEM image of the cycled electrode.

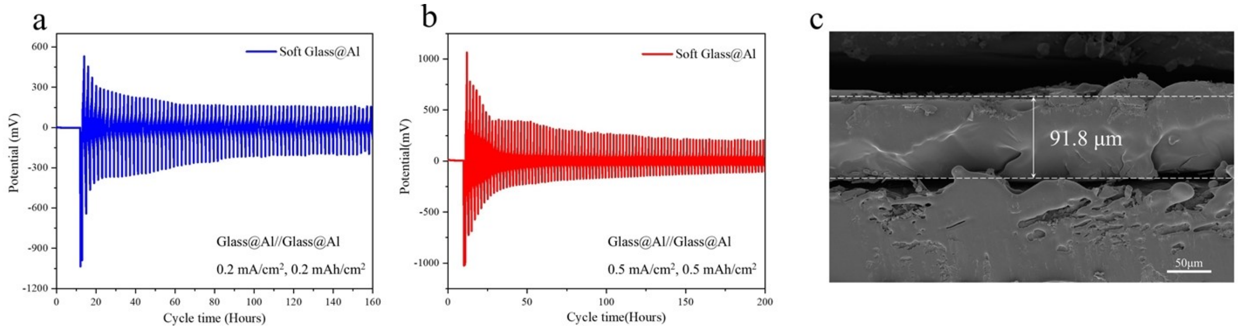

Figure S18. Long-term cycling performance and post-cycling characterization of ZnP-H_2Im@Al symmetric cells: (a) Cycling profiles at 0.2 mA/cm² and 0.2 mAh/cm², (b) profiles at 0.5 mA/cm² and 0.5 mAh/cm², (c) cross-sectional SEM image of the cycled electrode.

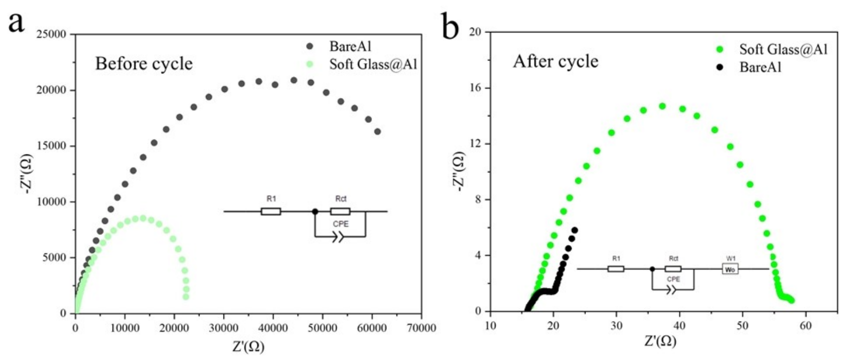

Figure S19. Electrochemical impedance spectra (EIS) of ZnP-H_2Im@Al//ZnP-H_2Im@Al symmetric cells and Al//Al symmetric cells: (a) before cycling and (b) after cycling.

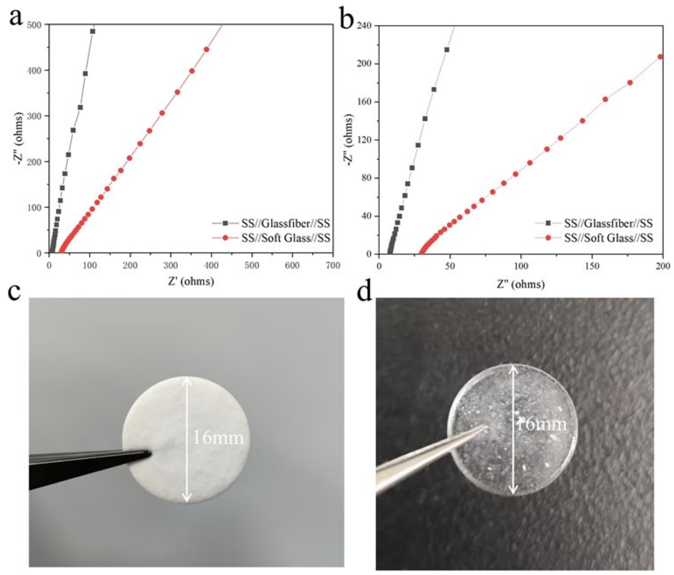

Figure S20. (a) EIS spectra of the SS//glass fiber//SS cell and SS//ZnP-H_2Im//SS cell, (b) magnified view of the EIS spectra; (c) photograph of the ZnP-H_2Im soft glass separator, (d) photograph of the glass fiber separator.

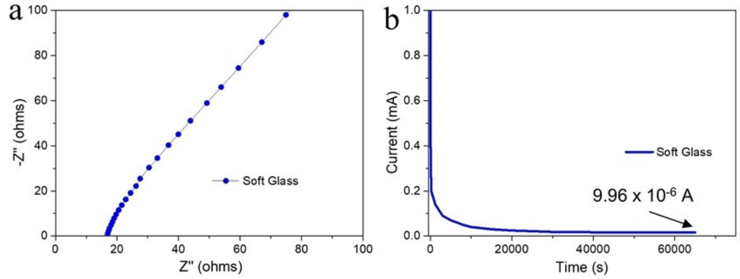

Figure S21. (a) Impedance spectra for total electronic conductivity of Soft Glass. (b) DC polarization curves for electronic conductivity of Glass at 0.01 V.

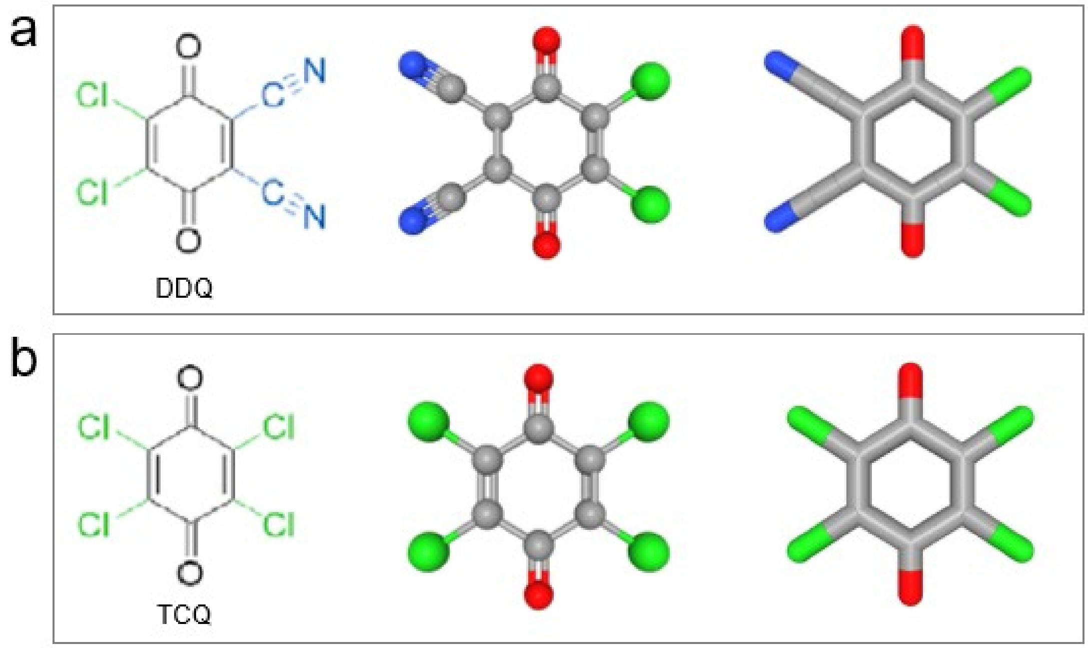

Figure S22. (a) Schematic diagram of the chemical structure of DDQ. (b) Schematic diagram of the chemical structure of TCQ.

Figure S23. Photograph of TCQ powder.

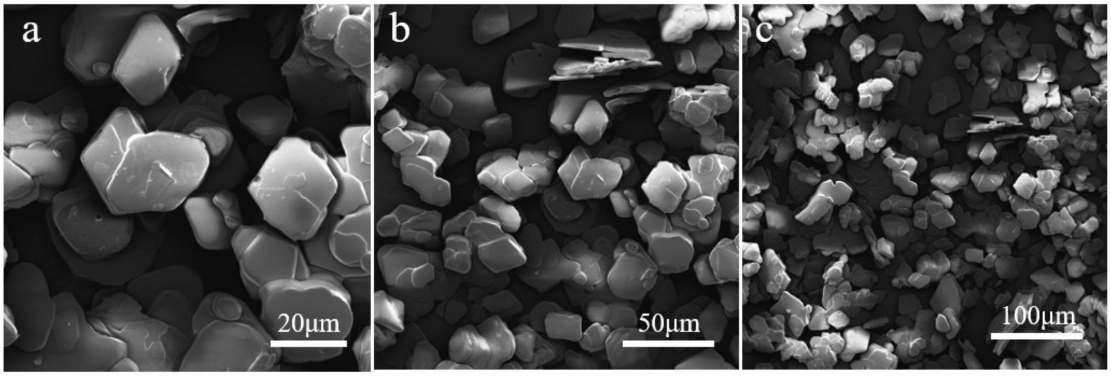

Figure S24. SEM image of TCQ powder.

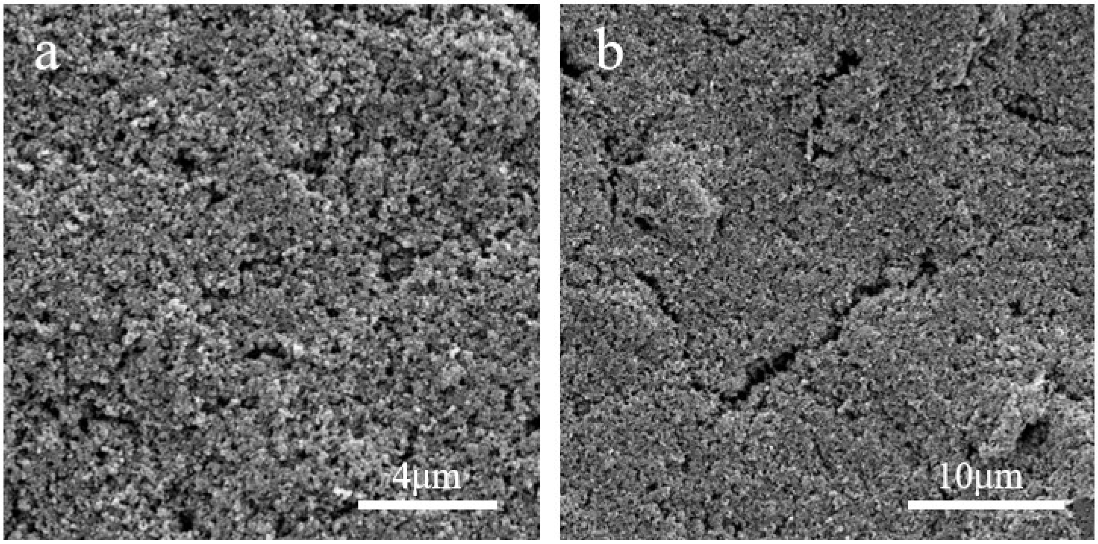

Figure S25. SEM image of the surface of the TCQ@Mo cathode.

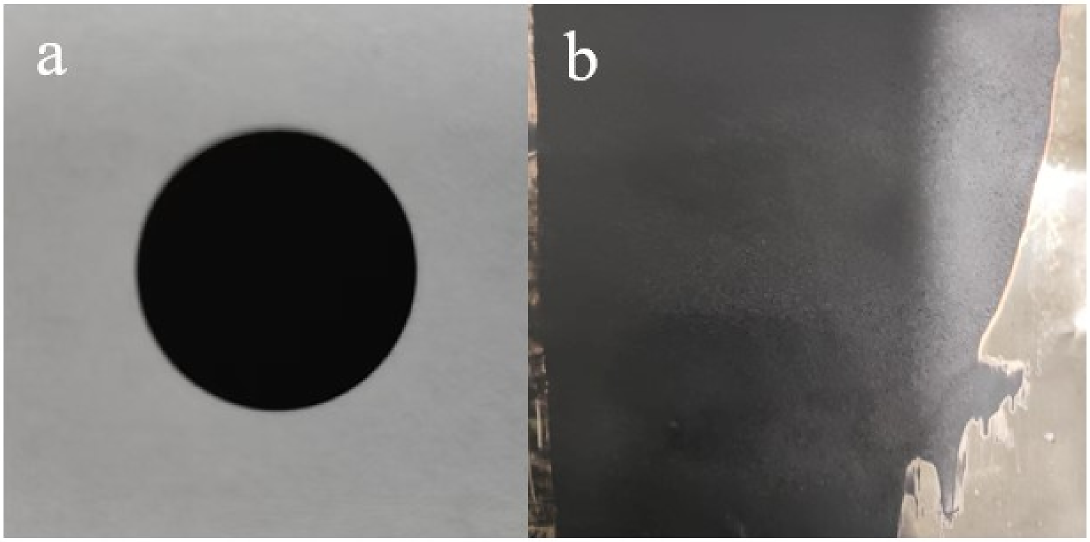

Figure S26. Photograph of the TCQ@Mo cathode electrode.

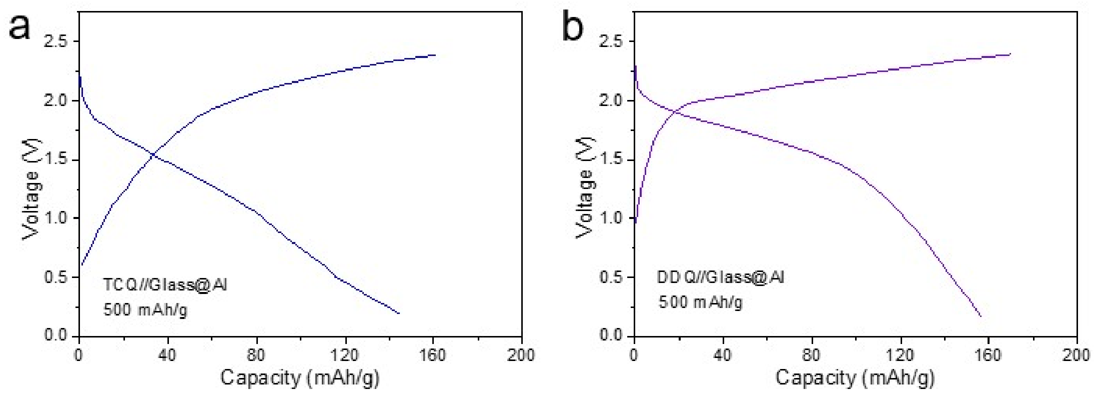

Figure S27. (a) Charge/discharge curves of the TCQ@Mo//ZnP-H_2Im@Al full cell. (b) Charge/discharge curves of the DDQ@Mo//ZnP-H_2Im@Al full cell.

Figure S28. Photograph of DDQ powder.

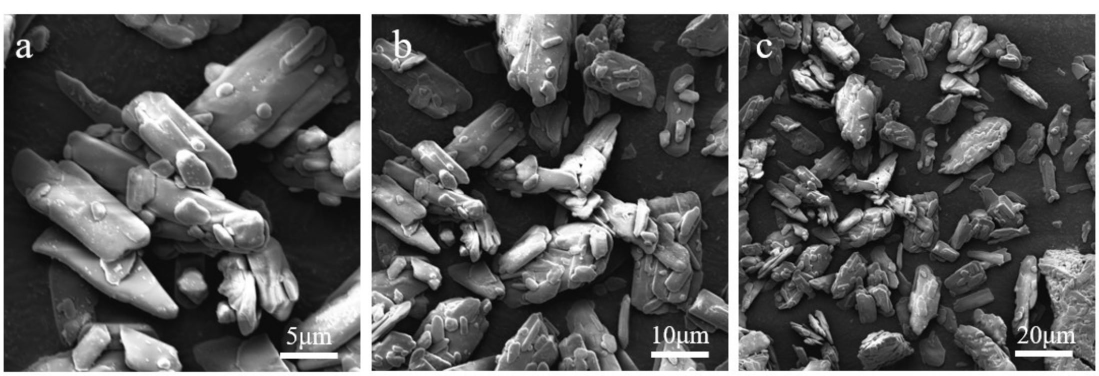

Figure S29. SEM image of DDQ powder.

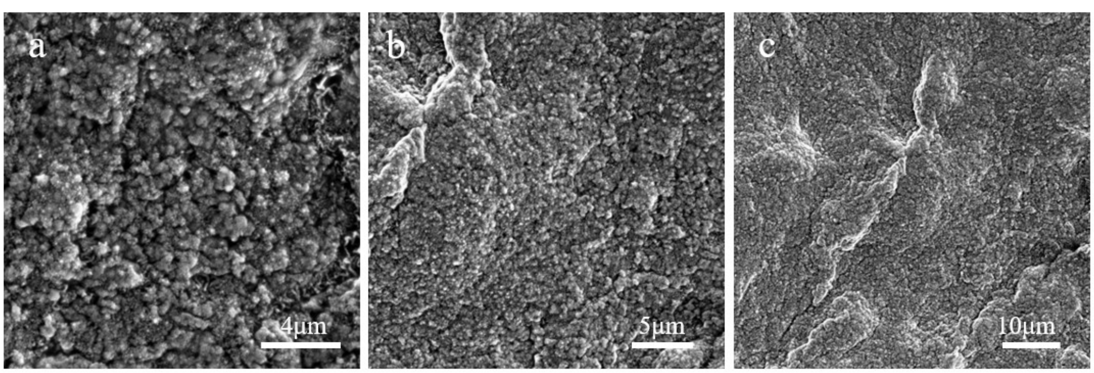

Figure S30. SEM image of the surface of the DDQ@Mo cathode electrode.

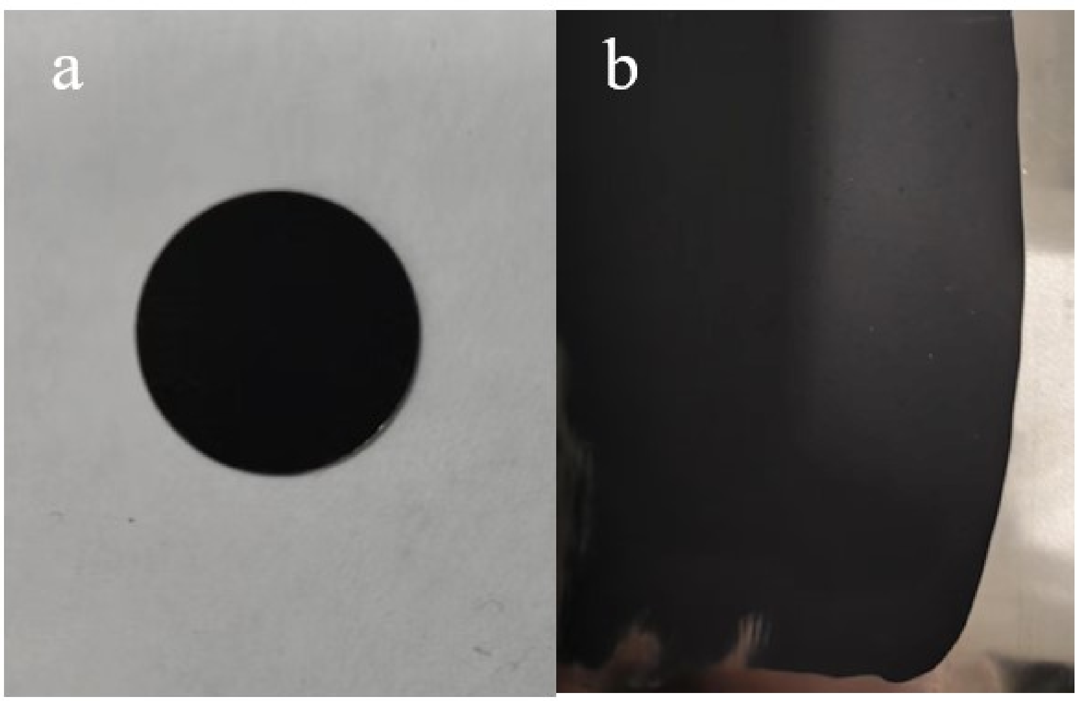

Figure S31. Photograph of the DDQ@Mo cathode electrode.

electrode	Electrolyte	Current density (mA/cm^2)/Areal capacity of Al deposition(0.5mAh/cm^2)	Life time(h)	Year	Ref.
Znp-H_2Im@Al	$AlCl_3$/[EMIm]Cl	0.5 / 0.5 0.2/0.2	10000 10000	--	This work
bareAl	$AlCl_3$/[EMIm]Cl	0.5 / 0.5 0.2/0.2	210 650	--	This work
Al soaked in electrolyte for 6 hours	$AlCl_3$/[BMIM]Cl	0.04/0.4	1200	2017	1
Zn-supported Zn− Al alloy	2 M $Al(OTF)_3$	0.2/0.2	1500	2020	2
Porous Al	$AlCl_3$/[EMIm]Cl	5/0.25	360	2020	3
NCRA	$AlCl_3$/[EMIm]Cl	0.5/0.5 1/1	300 300	2020	4
a patterned substrate composed of carbon fibres	$AlCl_3$/[EMIm]Cl	4/0.8 1.6/3.2 1.6/8	3600 3600 3600	2021	5

E-Al82Cu18	2M Al(OTF)$_3$	0.5 / 0.5	2000	2022	6
Al@a-Al	0.5 M $Al_2(SO_4)_3$	0.05/0.1	800	2022	7
SA-Co/NPCS	$AlCl_3$/[EMIm]Cl	0.4/5 0.4/10 40/0.4	3000 1000 1500	2023	8
Al	$AlCl_3$/[EMIm]Cl with CTAC additives	0.5/0.5 3/1	300 1200	2024	9

Table S1 Electrochemical Performance Comparison of ZnP-H_2Im@Al Symmetric Cells with Previously Reported Systems

Sample	Melting temperature（Tm）/℃	Synthesis time required/h	Mechanical properties	Year	Ref.
ZnP-H_2Im glass	160	20	Soft	--	This work
α-[Cu(ipim)] β-[Cu(ipim)]	185 146	115	--	15	10
ZIF-4 TIF-4	590 467	100 130	Hard	16	11
[Zn(im)1.62(5-Clbim)0.38](ZIF-76) [Zn(im)1.33(5-mbim)0.67] (ZIF-76-mbim)	451 471	130	hard	18	12
ZIF-62	440	160	Hard	20	13
Zn-P dmbIm Cd-P-dmbIm Cu-P-dmbIm Mn-P-dmbIm	176 172 166 162	11	soft	21	14
(TPrA)[Mn(dca)3]	271	150	Soft	21	15

(TPrA)[Fe(dca)3]	263				
(TPrA)[Co(dca) 3]	230				
Cobalt-ZIF-62	270	110	Hard	22	16
a_{gf}ZIF-62	378	100	Soft	23	17
ZIF-62	414	90	Hard		
MUV-24	482	100	Hard	23	18
G-Mg-adp	284	30	Hard	24	19
G-Mn-adp	238				

Table S2. Comparative Analysis of ZnP-H_2Im Glass Synthesis Conditions and Mechanical Properties with Prior Studies.

Sample	Cost (USD/kg)	toxicity	productivity	Waste disposal methods	Ref.
Znp-H_2Im	292	Low	95%	Electrocatalytic oxidation	This work
Zn-P-dmbIm	2065	low	90%	Electrocatalytic oxidation	20
MoO_3	21188	Medium	92%	Chemical precipitation method	21
$Ti_{0.95}\square_{0.05}O_{1.79}Cl_{0.08}(OH)_{0.13}$	616	Medium	88%	Chemical precipitation method	22
ZIF-62（Co）Crystal	7233	Medium	85%	Chemical precipitation method	23
$FeFe(CN)_6$	1921	Low	91%	Chemical precipitation method	24

CoHCF	767	Medium	83	Chemical precipitation method	25

Table S3 presents a comparative statistical table of ZnP-H_2Im soft glass and previously reported materials in lithium-ion and aluminum batteries, analyzing parameters including cost, toxicity, yield, and waste treatment methods.

References

1 F. Wu, N. Zhu, Y. Bai, Y. Gao and C. Wu, *Green Energy Environ.*, 2018, **3**, 71-77.

2 C. Yan, C. Lv, L. Wang, W. Cui, L. Zhang, K. N. Dinh, H. Tan, C. Wu, T. Wu, Y. Ren, J. Chen, Z. Liu, M. Srinivasan, X. Rui, Q. Yan and G. Yu, *J. Am. Chem. Soc.*, 2020, **142**, 15295-15304.

3 Y. Long, H. Li, M. Ye, Z. Chen, Z. Wang, Y. Tao, Z. Weng, S.-Z. Qiao and Q.-H. Yang, *Energ. Storage Mater.*, 2021, **34**, 194-202.

4 H. Jiao, S. Jiao, W.-L. Song, X. Xiao, D. She, N. Li, H. Chen, J. Tu, M. Wang and D. Fang, *Nano Res.*, 2021, **14**, 646-653.

5 J. Zheng, D. C. Bock, T. Tang, Q. Zhao, J. Yin, K. R. Tallman, G. Wheeler, X. Liu, Y. Deng, S. Jin, A. C. Marschilok, E. S. Takeuchi, K. J. Takeuchi and L. A. Archer, *Nat. Energy*, 2021, **6**, 398-406.

6 Q. Ran, H. Shi, H. Meng, S.-P. Zeng, W.-B. Wan, W. Zhang, Z. Wen, X.-Y. Lang and Q. Jiang, *Nat. Commun.*, 2022, **13**, 576.

7 C. Yan, C. Lv, B.-E. Jia, L. Zhong, X. Cao, X. Guo, H. Liu, W. Xu, D. Liu, L. Yang, J. Liu, H. H. Hng, W. Chen, L. Song, S. Li, Z. Liu, Q. Yan and G. Yu, *J. Am. Chem. Soc.*, 2022, **144**, 11444-11455.

8 L. Yao, S. Ju, G. Xia, D. Sun and X. Yu, *ACS Energy Lett.*, 2024, **9**, 253-261.

9 Y. Xie, X. Du, Y. Meng, Y. Liu, S. Wang, W. You, M. Liu, Y. Guo, Z. Liang and D. Li, *Energy Storage Mater.*, 2024, **70**, 103545.

10 Y.-J. Su, Y.-L. Cui, Y. Wang, R.-B. Lin, W.-X. Zhang, J.-P. Zhang and X.-M. Chen, *Cryst. Growth Des.*, 2015, **15**, 1735-1739.

11 T. D. Bennett, Y. Yue, P. Li, A. Qiao, H. Tao, N. G. Greaves, T. Richards, G. I. Lampronti, S. A. T. Redfern, F. Blanc, O. K. Farha, J. T. Hupp, A. K. Cheetham and D. A. Keen, *J. Am. Chem. Soc.*, 2016, **138**, 3484-3492.

12 C. Zhou, L. Longley, A. Krajnc, G. J. Smales, A. Qiao, I. Erucar, C. M. Doherty, A. W. Thornton, A. J. Hill, C. W. Ashling, O. T. Qazvini, S. J. Lee, P. A. Chater, N. J. Terrill, A. J. Smith, Y. Yue, G. Mali, D. A. Keen, S. G. Telfer and T. D. Bennett, *Nat. Commun.*, 2018, **9**, 5042.
13 Y. Wang, H. Jin, Q. Ma, K. Mo, H. Mao, A. Feldhoff, X. Cao, Y. Li, F. Pan and Z. Jiang, *Angew. Chem. Int. Ed.*, 2020, **59**, 4365-4369.
14 J. Li, J. Wang, Q. Li, M. Zhang, J. Li, C. Sun, S. Yuan, X. Feng and B. Wang, *Angew. Chem. Int. Ed.*, 2021, **60**, 21304-21309.
15 B. K. Shaw, A. R. Hughes, M. Ducamp, S. Moss, A. Debnath, A. F. Sapnik, M. F. Thorne, L. N. McHugh, A. Pugliese, D. S. Keeble, P. Chater, J. M. Bermudez-Garcia, X. Moya, S. K. Saha, D. A. Keen, F.-X. Coudert, F. Blanc and T. D. Bennett, *Nat. Chem.*, 2021, **13**, 778-785.
16 C. Gao, Z. Jiang, S. Qi, P. Wang, L. R. Jensen, M. Johansen, C. K. Christensen, Y. Zhang, D. B. Ravnsbæk and Y. Yue, *Adv. Mater.*, 2022, **34**, 2110048.
17 Z. Yang, Y. Belmabkhout, L. N. McHugh, D. Ao, Y. Sun, S. Li, Z. Qiao, T. D. Bennett, M. D. Guiver and C. Zhong, *Nat. Mater.*, 2023, **22**, 888-894.
18 L. León-Alcaide, R. S. Christensen, D. A. Keen, J. L. Jordá, I. Brotons-Alcázar, A. Forment-Aliaga and G. Mínguez Espallargas, *J. Am. Chem. Soc.*, 2023, **145**, 11258-11264.
19 M. Kim, H.-S. Lee, D.-H. Seo, S. J. Cho, E.-c. Jeon and H. R. Moon, *Nat. Commun.*, 2024, **15**, 1174.
20 L. Bai, Y. Xu, Y. Liu, D. Zhang, S. Zhang, W. Yang, Z. Chang and H. Zhou, *Nat. Commun.*, 2025, **16**, 3484.
21 H. Lahan and S. K. Das, *Journal of Power Sources*, 2019, **413**, 134-138.
22 X. Wu, N. Qin, F. Wang, Z. Li, J. Qin, G. Huang, D. Wang, P. Liu, Q. Yao, Z. Lu and J. Deng, *Energy Storage Mater.*, 2021, **37**, 619-627.
23 C. Gao, Z. Jiang, S. Qi, P. Wang, L. R. Jensen, M. Johansen, C. K. Christensen, Y. Zhang, D. B. Ravnsbæk and Y. Yue, *Adv. Mater.*, 2022, **34**, 2110048.
24 R. Bai, J. Yang, G. Li, J. Luo and W. Tang, *Energy Storage Mater.*, 2021, **41**, 41-50.
25 X. Yuan, X. Yuan, S. Zhang, P. Chen, X. Wu, J. Ye, L. Liu, L. Fu, T. Wang, K. I. Ozoemena and Y. Wu, *Adv. Energy Mater.*, 2024, **14**, 2302712.